Раздел первый

ФИЗИКА РАДИАЦИОННЫХ ПОВРЕЖДЕНИЙ И ЯВЛЕНИЙ В ТВЕРДЫХ ТЕЛАХ

ATOMIC DENSITY AT HIGH-ANGLE GRAIN BOUNDARIES IN TUNGSTEN

V.A. Ksenofontov, A.A. Mazilov, T.I. Mazilova, E.V. Sadanov, V.I. Sokolenko, V.N. Voyevodin, O.V. Dudka, I.M. Mikhailovskij
National Science Center "Kharkov Institute of Physics and Technology", Kharkov, Ukraine
E-mail: mikhailovskij@kipt.kharkov.ua

The oscillatory features of the atomic relaxation and the phenomenon of plane coalescence on high-angle grain boundaries in tungsten are studied by the methods of molecular statics and field ion microscopy. A nonmonotonic character of the variation of the atomic density in the near-boundary region is established. The strain field normal to the boundary plane is calculated and compared with the results obtained using the embedded-atom method in the reciprocal space. It is shown that the amplitude, period, and character of damping of the oscillations near grain boundaries can be described satisfactorily in the framework of the line forces model.

PACS: 61.16.Di; 61.72.Mm; 68.35.Bs

INTRODUCTION

A grain boundary dilatation significantly affects the kinetics of formation and migration of point defects, the interaction between lattice dislocations and grain boundaries [1-3]. This fundamental property of grain boundaries determines grain boundary energy and controls the response of polycrystals to an applied mechanical stress [4]. A theoretical analysis of the structure of the grain boundaries (GBs) on the basis of the continuum theory of dislocations made it possible to describe the basic properties of polycrystals. In a microscopic determination of the elastic stress fields in the neighbourhood of twins and symmetric grain boundaries one observes some features, which cannot be described in terms of the continuum theory of dislocations [1, 5-7]. As was shown in [1], the boundary expansion is caused by the localized short-range repulsion generated by atomic overlap in the unrelaxed state and is limited by the work done against the attraction across the interface. Strains are distributed in both grains, as to be expected for a coherent boundary coupled elastically. All kinds of GBs are characterized by an abrupt transition from maximum to minimum compression in the boundary. In the isolated dislocation case the lattice is in compression above the edge dislocation, to accommodate the extra half-plane, and, alternatively, below in expansion. However, as far as the shape of the grain-boundary elastic field is concerned, the local stress near steps does not show a pure alternating character typical of lattice dislocations and significant additional stresses are localized at the boundary plane [1, 6].

The evolution of the fine scale of the morphology of tilt GBs is driven by localized interface stresses. Regular periodic arrays of the grain-boundary microfacets are stabilized through relaxation displacements by the lines of force running along the axis of misorientation [1]. In addition to a generally accepted description of the variation of the stress field at the coherent near-twin boundary in terms of twinning dislocation, the interface stress includes Marchenko-Parshin linearly distributed surface forces [7, 8]. Localized line forces may be responsible for the increase of the temperature of the superconducting transition in nanolayer of metal near the coherent (dislocation-free) twin boundaries [9, 10]. At the coherent twin boundaries, the near-interface relaxation of the atomic layers displays an oscillatory behavior with an exponential decay into the interior of the metal [1, 7]. An analogous character of the displacements of the atomic planes has been observed in the neighborhood of certain special symmetric boundaries in metals with the fcc lattice and covalent crystals [1, 11].

Clearing-up the nature of this GB phenomenon becomes an entry point for determination of the stress field near the grain boundary. The origin of the oscillations of the interplanar distances in the neighborhood of grain boundaries in some cases is due to the features of the local bending of the atomic planes in the neighborhoods of the cores of grain-boundary dislocations [1]. However, there are no structural grain-boundary dislocations present neither at the coherent twin boundary nor at other symmetric special boundaries with a high density of coincident sites. The nature of this strain profile was also traced to the Friedel oscillations of the electron density which drive the atom to relax in such an oscillatory mode [11, 12]. The character of damped oscillations is determined by many macroscopic and microscopic parameters which characterize the structure and microtopography of grain boundaries. This circumstance severely hampers the elucidation of the physical nature of this phenomenon. In present study, we investigate the oscillatory behavior of the density in the vicinity of twin and grain boundaries in tungsten. Revealed large oscillatory

multilayer relaxations could be rationalized in the framework of the theory of elasticity.

MATERIAL AND METHODS

We use the N-body embedded atom method developed for tungsten by Foiles [13]. Most methodical details of the calculation of the atomic configuration of the grain boundaries were described elsewhere [14, 15]. The Sutton version [16] of the variational calculation method in the reciprocal space is applied, and the electron density associated with the surrounding atoms is determined by the Fourier transform of the electron density. To calculate the energy of the relaxed twin boundary, the contributions to the binding energy of all atomic planes of a bicrystal are added. The relaxed structure corresponds to an infinitely extended bicrystal in the boundary plane free of macroscopic stresses. The relaxed configuration of the calculation block is determined by the molecular statics method by minimizing the energy, including the dilatation deformation with respect to the grain translations in the boundary plane and the local individual displacements of the atomic planes. The energy minimization was carried out using the conjugate gradient method. The atoms are initially located according to their positions in the coinciding-site lattice. The *y* axis is normal to the plane of the boundary and the *z* axis is taken to be parallel to the tilt axis [110].

For the field-ion microscopy (FIM), needle-shaped specimens with a radius of curvature of 10-100 nm were prepared by electrochemical polishing from 0,15 mm tungsten wire of 99,98 at.% purity (0,01 at.% Si, 0,002 at.% Fe, 0,005 at.% Mo), which had been manufactured by drawing metal-ceramic rods at 670…770 K. The wire had a fibrous structure with an average fiber diameter about 250 nm. The details of a field-ion microscope used were described elsewhere [17]. The background pressure was about 10^{-7} Pa and as an imaging gas, helium at a pressure of 10^{-3} Pa was used. After mounting in the microscope, the nanotip surface was cleaned and polished by the methods of field desorption and controlled field evaporation. We studied the Σ3 {111} <110> tilt twin boundary and Σ9 $(1\bar{1}4)$ 38,9° [110] tilt grain boundary. There Σ is the inverse density of coinciding sites. Due to their unusual properties, grain boundaries with low-Σ coincidence site lattices, in particular Σ3 and Σ9 boundaries play a special role in the grain boundary engineering. Most studies of grain boundary structure have focused on face-centred cubic materials which form annealing twins. In spite of the technological importance of body-centred cubic (bcc) refractory metals only few facts are known about atomic structure of the Σ3 {111} <110> twin boundary [1, 18, 19].

RESULTS AND DISCUSSION

Fig. 1,a shows the relaxed atomic structures of the tilt twin boundary Σ3 {111} <110>. Note that this boundary can be equally defined as a vicinal boundary to the Σ3 {211} <110> singular boundary (i.e. the coherent twin boundary). The initial incoherent twin boundary configuration is characterized by the presence of strong repulsive and attractive forces. The shortest distance between the atoms in the planes on both sides of the boundary is very small (1,83 Å), whereas the distance between the second nearest atomic planes is large (3,66 Å). The solid and open circles correspond to the atomic positions in two nonequivalent {110} plane. The calculated displacements normal to the grain boundary for the {111} are obtained by subtracting the unrelaxed atomic positions normal to the boundary plane from the relaxed atomic positions. The initial atomic configuration of the Σ3 (111) boundary structure in tungsten can be described as a succession of (111) hexagonal atomic layers: …CBACB**A**BCABC… where the GB plane is marked by **A**. The interplanar distances corresponding to a minimum of energy were varied, whereas the structure within the (111) planes were left unchanged. One can see that the largest displacement occurs at the first layer parallel to the grain boundary. This gives rise to the rippling effect close to the boundary interface similar to that observed in the free surface [20]. The relaxation of the atomic structure of the incoherent twin boundary is accompanied by a decrease in the internal energy from 18,0 to 3,45 J/m^2. The relaxed structure is characterized by the presence of dilatation perpendicular to the grain boundary with subsequent compression. Fig. 1,b shows the displacements of atomic layers {111} normal to the twin boundary in fully relaxed state as a function of the distance from the boundary (in units of n, where n is the number of atomic layer away from the boundary plane). In most cases, the vast majority of the grain-boundary dilatation is taken up right at the boundary plane. But in the case of the {111} incoherent twin boundary although a considerable expansion is taken up at the boundary plane (n = 0) there are large oscillations in the interlayer spacing that decay exponentially away from the twin boundary.

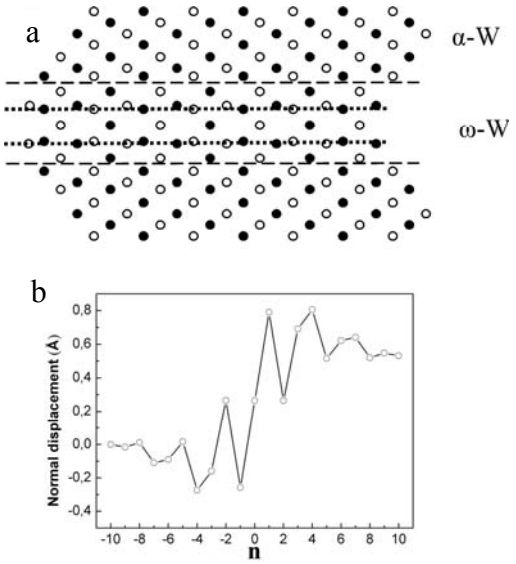

Fig. 1. Relaxed atomic structure of the Σ3 {111} <110> incoherent twin boundary (a) and the equilibrium normal displacements of the {111} atomic layers (b)

The structure of the twin boundary can be characterized by analyzing the spacing of the adjacent (111) planes as function of the distance from the boundary plane and comparing it with the bulk value

d_{111} = 0,914 Å (Fig. 2). The GB-relaxation calculations show that the interplanar distances oscillate as a function of distance from the GB plane with the amplitude of oscillations gradually decreasing. A remarkable feature of the Σ3 <110> {111} GB relaxation is that the separation of the 2nd and 3rd atomic layers is a little part of the (111) interplanar distance in the bulk tungsten (0,32 versus 0,914 Å). The damping oscillations of the interlayer spacing are generated by the alternation of attractive and repulsive forces near the twin boundary. The rigid displacement of the neighboring grains at the boundary along the <110> direction is absent, in agreement with the mirror symmetry of the bicrystal with respect to the {110} plane. The twin boundary is wide and symmetric in contrast to the Σ3 coherent twin boundary in the fcc metals [1]. The neighboring atomic planes in the immediate vicinity of the twin boundary Σ3 {111} <110> coalesce with the formation of the atomically smooth flat monolayer with the hexagonal close-packed structure (see Fig. 1,a). The positions of the atoms after relaxation near the core of the {111} inclined symmetric twin boundary correspond to the structure of the ω-phase [21] usually observed in pure Ti, Zr, and Hf. The ω-structure is obtained from the bcc lattice by the supposition of the longitudinal displacement waves in the <111> direction, which induce the collapse of alternating pairs of the {111} bcc planes. The structure of the ideal (commensurate) ω-phase with hexagonal symmetry can be represented by alternating of single and double {111} bcc planes. The width of the grain-boundary ω-phase found in computer experiments is equal to seven {111} bcc atomic planes. Our results are in accord with results of the determination of the electronic densities at similar interfaces. The electronic densities of states of atoms on the Σ3 <110> {111} GB bcc metals are very much like that for omega-phase [22].

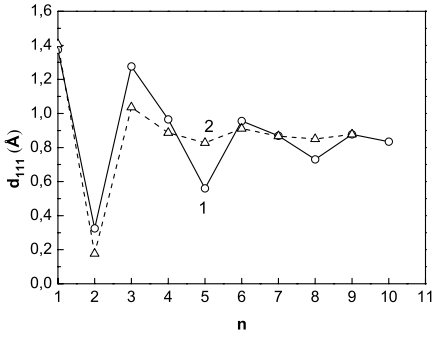

Fig. 2. Damped oscillations of interplanar distance near the Σ3 <110> {111} twin boundary. The line (1) represents the atomistic simulation and line (2) analytical continuum model

A change in the excess internal energy with the distance from the incoherent twin boundary in the relaxed state is also nonmonotonic [7]. The excess energy as a function of {111} plane number n is maximal not at the geometric boundary center (n = 0), but in the nearest atomic plane. The central atomic layer at the Σ3 {111} [110] boundary has negative excess energy (–0.50 J/m^2). This means that the atomic sites in the central plane of the twin boundary are characterized by a binding energy higher than that in the bulk of the perfect crystal. The energies of the atoms in two sites of the sublattices of neighboring coalesced layers are significantly different and are equal to 1,78 and 0,90 J/m^2. It should be noted that while a direct comparison with the experiments is not possible in case of the twin relaxation, the extension of relaxation waves of about ten atomic layers observed in a recent atomistic simulation is in qualitative and quantitative agreement with results obtained in experiments on electron-phonon interactions near the twin boundaries in superconductors [9, 10].

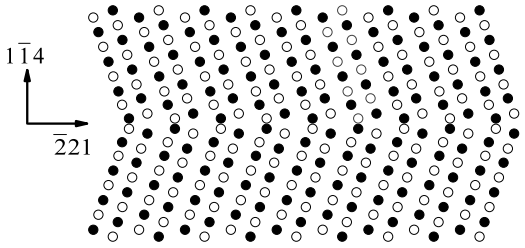

Fig. 3. Atomic structure of the Σ9 $(1\bar{1}4)$ 38,9° [110] tilt grain boundary. The white and black circles denote atoms on the two (110) planes in each [110] period

Fig. 3 shows the atomic structures of the Σ9 $(1\bar{1}4)$ 38,9° [110] tilt grain boundary. The strain field of the Σ9 grain boundary is similar to those found near the Σ3 {111} [110] symmetric twin boundary. For this grain boundary, we find that the relaxed interlayer strain perpendicular to the grain boundary shows an oscillatory behavior with a rapidly decaying profile with increasing distance from the boundary plane (Fig. 4). The interlayer strain normal to the grain boundary oscillates with increasing distance from the grain boundary. This configuration occurs after the lattices of the adjacent grains undergo rigid shift along the $[\bar{2}21]$ direction by a distance of 2,56 Å followed by shifts of atomic planes. The maximum excess energy in the core of the boundary is 0,75 eV/atom. The core configurations of the Σ9 38,9° [110] grain boundary in this state of rigid body translation the two planes coalesced completely at the core center. The reason for the spatial oscillations of the spacing between atomic planes in the vicinity of grain boundaries is widely believed to be associated with the curving of atomic planes near the cores of grain-boundary boundary edge dislocations [1]. This model allows one to qualitatively describe density oscillations and coalescence of grain-boundary atomic planes. However, the Σ9 $(1\bar{1}4)$ 38,9° [110] tilt boundary, as well as other symmetrical commensurate grain boundaries with a high density of coincident sites, has no structural grain-boundary dislocations. At GB steps, repulsive short-range forces operate because of the interaction between the adjacent grains. In the vicinity of atoms with a higher excess energy in the boundary with a translational shift of 2,56 Å, the compression stress component σ_{yy} normal to the surface, is equal to 30 GPa; i.e., it is of the order of 0,1E, where E is Young's modulus. The repulsive short range forces operating mainly in the vicinity of

relatively close-packed [110] chains of atoms produce a grain-boundary dilatation, the limiting value of which is determined by the work of the attractive long-range forces acting between the atoms of the adjacent grains.

A crystallographic and geometrical analysis of the symmetrical commensurate grain boundary considered reveals that these tilt boundaries can be considered as a dislocation-free staircase-like surface with terraces being parallel to the singular {112} faces. Analysis of the features of the compression stress in the neighborhood of twin and grain boundaries allows one to replace the complex pattern of interaction of adjacent crystallites by periodic rows of parallel line forces for describing the elastic strain field [7, 23]. The boundary dilatation caused by the localized repulsion generated by partial atomic overlap is limited by the long-range attraction across the boundary. A spike of increased compression, with respect to the matrix, obvious above the boundary steps with a less pronounced expansion below can be described as in terms of lines of elastic compression forces on a flat surface [7].

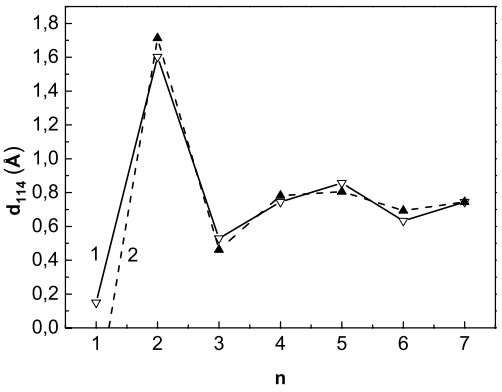

Fig. 4. Oscillations of interplanar distance near the Σ9 $(1\bar{1}4)$ 38,9° [110] tilt grain boundary. The solid and dotted lines represent the atomistic simulation and analytical model, respectively

We will replace the complex force pattern of interaction between adjacent grains by the periodic arrays of line forces at elastic analysis of the GB relaxation. Linear distributed forces are assumed to be localized near close-packed atomic chains on the grain boundary, which are characterized by an excess energy. Each of the grains is considered as an elastic continuum bounded by a plane surface. The distance Λ along the *x* axis between the line forces is equal to the GB step separation. The length Λ of the steps parallel to the axis of misorientation is determined by the translational symmetry of the boundary and is usually equal to the period vector and they are the same in all materials with a bcc lattice. However, some periodic [110] tilt boundaries in metal belong to centered type with the base-centered plane parallel to the boundary. There are two coincident sites in each period of the boundary and the atomic structure of the boundary repeats in each half-period except for a relative shift of a/2[110]. The spacing Λ between steps on the Σ9 $(1\bar{1}4)$ 38,9° [110] tilt boundary is $a/2[\bar{2}21]$ (the half-period of the lattice in the direction perpendicular to the tilt axis). At these steps, repulsive short-range forces operate because of the interaction between the adjacent grains.

In order to obtain qualitatively the main features of the GB relaxation, we shall present the solution of the line forces problem by making the simplifying assumption that the compression line forces *F* are partially compensated by continuously distributed surface forces (Fig. 5). The forces *F*, uniformly distributed over the tilt axis *z*, are directed along the *y* axis, normal to the plane surface bounding the elastic half-space.

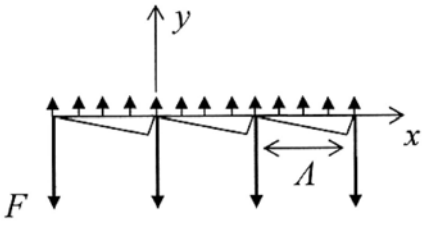

Fig. 5. Schematic representation of the line forces model for a vicinal grain boundary which consists of parallel equidistant steps. The line force spacing Λ is equal to interstep distance.

Single linear distributed force acting on the plane surface bounding the elastic half-space produces a strain field [24]

$$\sigma_{xx} = -\frac{2F}{\pi}\cdot\frac{x^2 y}{r^4}; \quad (1a)$$

$$\sigma_{yy} = -\frac{2F}{\pi}\cdot\frac{y^3}{r^4}; \quad (1b)$$

$$\sigma_{zz} = -\frac{2\nu F}{\pi}\cdot\frac{y}{r^2}, \quad (1c)$$

where *F* is the applied force per unit length and *ν* is the Poisson ratio, $r = \sqrt{x^2 + y^2}$. The appropriate strains can be obtained from Hooke's law:

$$\varepsilon_{xx} = \frac{F\cdot y}{\pi\cdot G r^2}(\nu - \frac{x^2}{r^2}); \quad (2a)$$

$$\varepsilon_{yy} = \frac{F\cdot y}{\pi\cdot G r^2}(\nu - \frac{y^2}{r^2}); \quad (2b)$$

$$\varepsilon_{zz} = 0. \quad (2c)$$

Here *G* is shear modulus.

The strain of uniform array of parallel line forces may be calculated using the same sums used in determination of the near-surface strain field [25] from the elastic fields of individual line forces:

$$\varepsilon_{yy} = -\frac{F}{G\pi}\sum_{n=-\infty}^{\infty}\left[\frac{y\nu}{(x+n\Lambda)^2 + y^2} - \frac{y^3}{((x+n\Lambda)^2 + y^2)^2}\right]. \quad (3)$$

Far from the surface ($y >> \Lambda$), arrays of line forces shown in Fig. 3 would result in a uniform compression $\sigma_{yy} \to F/\Lambda$. In this model, continuously distributed surface forces guarantee that remote from the interface material will be unstrained. Such a surface force is equivalent to a negative pressure – *F*/Λ. The elastic displacements are found by integration of Eq. (3) with respect to *y* and subtraction of the far-field displacements due to continuously distributed attractive forces:

$$U_y = \frac{F}{4\pi G}\{Y\frac{\cos(X)-\exp(-Y)}{\cosh(Y)-\cos(X)}+ \quad (4)$$
$$+2(1-\nu)[Y-\ln(2(\cosh(Y)-\cos(X)))]\},$$

where $X = 2\pi x/\Lambda$ and $Y = 2\pi y/\Lambda$.

The local values of the spacing between atomic layers i and i+1 are determined from Eq. (4) as $d_i = d + (U_{i+1} - U_i)$. The relaxing shifts of the atomic layers perpendicular to the grain boundary can be found if the atomic displacements in adjacent planes parallel to the tilt boundary are given. For the Σ9 $(1\bar{1}4)$ 38,9° [110] tilt boundary, the displacements of atoms in the i-th plane in the x direction can be written as [26]

$$x_i - x = (2i/9)[\bar{2}21]. \quad (5)$$

Fig. 4 shows the relative relaxing shift of the planes calculated within the continuum model as a function of the distance from the Σ9 $(1\bar{1}4)$ boundary (curve *2*). Since the linear distributed forces cannot be found in the framework of the elasticity theory, we used those values of F that gave the best fit of the calculated data to the experimental curve.

The resolution of recent microscopic techniques is insufficient to direct detection of the grain boundary oscillations of atomic layers. However, these experimental methods can ensure additional information on relaxed atomic structures of GBs. The Σ3 [110] incoherent twin boundaries can be frequently revealed by FIM within wire manufactured by drawing. Deformation twins have been observed in tungsten which macroscopically appeared to be in arbitrary orientation. Taking into account that the FIM image is projected stereographically and using standard graphical techniques, the specimen shown in Fig. 6 is found to contain a twin boundary with misorientation angle corresponds to an additional 3,5° tilt component from the exact Σ 3 coincidence. Thus, within the limits of experimental error of the FIM method of indirect magnification [27, 28] (~ 0,1 Å) it is concluded that there is no in-plane (lateral) component of rigid body displacement parallel to the [110] rotation axis.

FIM observations of the specimens showed that, as distinct from the grain boundaries with $\Sigma > 3$, the incoherent twin boundary is not subjected to preferential field evaporation. On the contrary, the phenomenon of preferential retaining during field evaporation takes place at the Σ3 <110> {111} twin boundary.

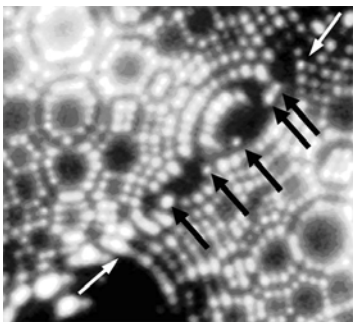

Fig. 6. Field ion micrographs of the Σ3 <110> twin boundary in tungsten shown by the white arrows. The black arrows show the atoms corresponding to the central {111} atomic layer of the boundary

Atoms which are preferentially retained through evaporation occupy prominent sites on the {211} and {321} planes in the central part of the boundary (indicated by black arrows in Fig. 6).

An analogical result was obtained at the Σ9 (114) 38,9° [110] tilt grain boundary (see Fig. 7). The cores of most of the large-angle boundaries have a reduced density and exhibit a tendency toward preferential field evaporation [27]. This effect is seen, in particular, in a decrease in the surface density of the imaged atoms along the track of grain boundaries. At special boundaries, an inversion of the contrast was observed in certain stages of the evaporation of atoms.

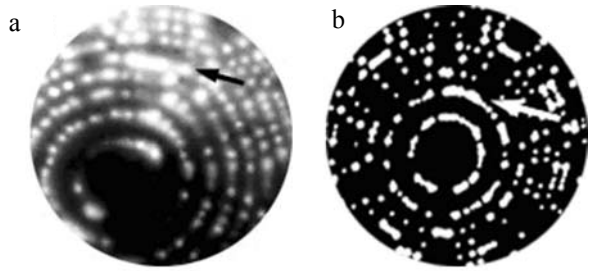

Fig. 7. Experimental (a) and simulated (b) FIM images of the Σ 9 grain boundary shown by arrows

Close-packed atomic chains of elevated brightness, oriented along the track of a boundary Σ9, were observed (Fig. 7,a). Analysis of ion micrographs recorded in succession during atom-by-atom field evaporation showed that local planar boundary regions with an elevated density may be responsible for the occurrence of a chain of atoms with an elevated brightness. Fig. 7,b shows for comparison a model image of a bicrystal containing the Σ9 (114) 38,9° [110] boundary. A numerical simulation was carried out in the approximation of a geometric model of thin shells [27, 28]. One of the atomic planes oriented parallel to the plane of the boundary has a doubled atomic density. Close-packed chains of atoms in the model images were observed during the stages of the field evaporation corresponding to a coincidence of the surface atomic steps with the track of the plane of the double-density boundary ($d_{114} \rightarrow 0$ at the center of the grain boundary shown in Fig. 4). Taken as a whole, the lattice correspondence and strong energetic heterogeneity in the core region of twin boundary revealed by computer simulations are consistent with the FIM images of the incoherent twin boundary.

CONCLUSION

The elastic field near the grain boundaries is calculated and compared with the results obtained using the embedded-atom method in the inverse space. Comparison between results of atomistic calculations and data obtained by theory of elasticity showed that the model of linearly distributed surface forces can give a satisfactory quantitative description of the oscillatory character of the multilayer atomic relaxation and the phenomenon of plane coalescence on grain and incoherent twin boundaries. The oscillatory relaxation profiles were observed for the local boundary dilatation. The simulated structures are consistent with the FIM images of the grain boundaries, which reveal the lattice

correspondence and strong energetic heterogeneity in the core region of twin boundary. The analytical treatment can be used to capture qualitatively the main features of the numerical findings on the GB relaxation: the amplitude, period, and character of damping of the oscillations. The structural origin of the multilayer oscillations is the grain boundary version of the terrace-ledge model for free surfaces.

We thank L.S. Shvindlerman and N. Wanderka for stimulating discussions and comments. This work was performed under the auspices of the National Academy of Sciences of the Ukraine and the Deutsche Forschungsgemeinschaft.

REFERENCES

1. A.P. Sutton, R.W. Balluffi. *Interfaces in crystalline materials.* Oxford: Clarendon, 1995, 819 p.
2. Q. Zhu, C.M. Sellars, H.K.D.H. Bhadeshia. Quantitative metallography of deformed grains // *Mater. Sci. Techn.* 2007, v. 23, p. 757-766.
3. G. Salishev, S. Mironov, S. Zherebtsov, A. Belyakov. Changes in misorientations of grain boundaries in titanium during deformation // *Mater. Charact.* 2010, v. 61, p. 732-39.
4. L.S. Shvindlerman, G. Gottstein. Unexplored topics and potentials of grain boundary engineering // *Scripta Mater*. 2006, v. 54, p. 1041-1045.
5. M. Sennour, S. Lartigue-Korinek, Y. Champion, M.J. Hÿtch. Local strain analysis in twin boundaries in ultrafine grained copper // *J. Mater. Sci.* 2008, v. 43, p. 3806-3811.
6. M.J. Hÿtch, J.-L. Putaux, J. Thibault. Stress and strain around grain-boundary dislocations measured by high-resolution electron microscopy // *Phil. Mag*. 2006, v. 86, p. 4641 - 4656.
7. T.I. Mazilova, I.M. Mikhailovskij, E.I. Lygovskaja. Fine structure of coherent twin boundaries in metals // *Low. Temp. Phys*. 2000, v. 26, p. 920-922.
8. V.I. Marchenko, A.Ya. Parshin. Elastic properties of the crystal surface // *Sov. Phys. JETP*. 1980, v. 52, p. 129-131.
9. A.V. Khotkevich, I.K. Yanson, M.B. Lazareva, V.I. Sokolenko, Ya.D. Starodubov. Effect of coherent twin boundaries on the electron-phonon interaction in single crystals of tin // *Pysica B.* 1990, v. 165-166, p. 1589-1590.
10. V.I. Sokolenko, Ya.D. Starodubov. Effect of crystal lattice defects on Tc of transition metals (a review) // *Low. Temp. Phys.* 1993, v. 19, p. 675-696.
11. M. Shiga, M. Yamaguchi, H. Kaburaki. Structure and energetics of clean and hydrogenated Ni surfaces and symmetrical tilt grain boundaries using the embedded-atom method // *Phys. Rev. B.* 2003, v. 68, p. 245402-8.
12. G. Lu, N. Kioussis. Interaction of vacancies with a grain boundary in aluminum: A first-principles study // *Phys. Rev. B*. 2001, v. 64, p. 024101-7.
13. S.M. Foiles. Interatomic interactions for Mo and W based on the low-order moments of the density of states // *Phys. Rev. B*. 1993, v. 48, p. 4287-4298.
14. I.M. Mikhailovskij, N. Wanderka, V.A. Ksenofontov, T.I. Mazilova, E.V. Sadanov, A.A. Mazilov. The ω structure of the lateral twin boundary in tungsten // *Phil. Mag. Lett.* 2007, v. 87, p. 743-750.
15. V.I. Gerasimenko, T.I. Mazilova, I.M. Mikhailovskij. Analytical model of rigid relaxation of grain boundaries in metals // *The Physics of Metals and Metallography*. 2001, v. 91, p. 335-339.
16. A.P. Sutton. An analytic model for grain-boundary expansions and cleavage energies // *Phil. Mag. A.* 1991, v. 63, p. 793 - 818.
17. I.M. Mikhailovskij, G.D.W. Smith, N. Wanderka, T.I. Mazilova. Non-kinkwise field evaporation and kink relaxation on stepped W(112) surface // *Ultramicroscopy*. 2003, v. 95, p. 157-163.
18. D. Fuks, K. Mundim, V. Liubich, S. Dorfman. Nonempirical simulations of Σ3 <111> tungsten grain boundary with boron atoms // *Surf. Rev. Lett.* 1999, v. 6, p. 705-718.
19. K. Mundim, S. Dorfman, D. Fuks. Decohesion of Sigma (3) (111) grain boundary in tungsten with boron interstitial // *Surf. Rev. Lett.* 2003, v. 10, p. 227-232.
20. P. Müller, A. Saúl. Elastic effects on surface physics // *Surf. Sci. Rep.* 2004, v. 54, p. 157-258.
21. R. Ahuja, J.M. Wills, B. Johansson, O. Eriksson. Crystal structures of Ti, Zr, and Hf under compression: Theory // *Phys. Rev. B.* 1993, v. 48, p. 16269-16279.
22. G.L. Krasko, G.B. Olson. Effect of hydrogen on the electronic structure of a grain boundary in iron // *Solid State Comm*. 1991, v. 79, p. 113-117.
23. I.G. Rasin, S. Brandon. Assigning physical significance to the diffuse interface between terraces in phase-field modeling of steps on crystal surfaces: modeling step-step interaction // *J. Mater. Sci.* 2009, v. 44, p. 5980-5989.
24. L.D. Landau, E.M. Lifshitz. *Course of theoretical physics*. New York: "Pergamon", 1986, 560 p.
25. D.J. Srolovitz, J.P. Hirth. Elastic analysis of the energy and relaxation of stepped surfaces // *Surf. Sci.* 1991, v. 255, p. 111-119.
26. T.I. Mazilova, I.M. Mikhailovskij. Rigid-body translations of atomic planes at symmetric grain boundaries // *Crystallogr. Rep.* 1997, v. 42, p. 729-734.
27. M.K. Miller, A. Cerezo, M.G. Hetherington, G.D.W. Smith. *Atom-probe field ion microscopy*. Oxford: Oxford University Press, 1996, 509 p.
28. V.M. Azhazha, I.M. Neklyudov, V.A. Ksenofontov, T.I. Mazilova, I.M. Mikhailovskij, E.V. Sadanov, A.A. Mazilov. Field-ion microscopy observations and atomistic simulations of rigid-body shifts at tilt grain boundaries in tungsten // *Surf. Rev. Lett.* 2008, v. 15, p. 557-565.

Статья поступила в редакцию 09.02.2011 г.

АТОМНАЯ ПЛОТНОСТЬ БОЛЬШЕУГЛОВЫХ ГРАНИЦ ЗЕРЕН В ВОЛЬФРАМЕ

В.А. Ксенофонтов, А.А. Мазилов, Т.И. Мазилова, Е.В. Саданов, В.И. Соколенко, В.Н. Воеводин, О.В. Дудка, И.М. Михайловский

Методами молекулярной статики и полевой ионной микроскопии изучены явление коалесценции атомных плоскостей и осциллирующий характер атомной релаксации на большеугловых границах зерен в вольфраме. Установлен немонотонный характер изменения атомной плотности в приграничной области. Рассчитаны поля напряжений, нормальные плоскости границы, и проведено сравнение с результатами, полученными с использованием метода погруженного атома в обратном пространстве. Показано, что амплитуда, период и характер затухания осцилляций вблизи границы могут быть удовлетворительно описаны в рамках модели линейных сил.

АТОМНА ГУСТИНА ВЕЛИКОКУТОВИХ МЕЖ ЗЕРЕН В ВОЛЬФРАМІ

В.О. Ксенофонтов, О.О. Мазілов, Т.І. Мазілова, Є.В. Саданов, В.І. Соколенко, В.М. Воєводін, О.В. Дудка, І.М. Михайловський

Методами молекулярної статики і польової іонної мікроскопії вивчені явища коалесценції атомних площин і характер атомної релаксації, який осцилює на великокутових межах зерен у вольфрамі. Встановлено немонотонний характер зміни атомної густини в примежовій області. Розраховані поля напруг, які нормальні площини межі, і проведено порівняння з результатами, отриманими з використанням методу зануреного атома в зворотному просторі. Показано, що амплітуда, період і характер загасання осциляцій поблизу межі можуть бути задовільно описані за допомогою моделі лінійних сил.